Original Article | Cardiovascular Imaging

eISSN 2005-8330
https://doi.org/10.3348/kjr.2025.1614
Korean J Radiol 2026;27(6):532-542

Korean Journal of Radiology
KJR

Opportunistic Assessment of Coronary Artery Calcium Volume and Density From Non-Electrocardiogram-Gated Chest CT Using Artificial Intelligence: Prognostic Implications in a Screening Cohort

Na Young Kim[1], Yun-Hyeon Kim[2], Jong Eun Lee[3], Young Joo Suh[1]

[1]Department of Radiology, Research Institute of Radiological Science, Severance Hospital, Yonsei University College of Medicine, Seoul, Republic of Korea
[2]Department of Radiology and Biomedical Engineering, Chonnam National University Hospital, Chonnam National University Medical School, Gwangju, Republic of Korea
[3]Department of Radiology and Research Institute of Radiology, Asan Medical Center, University of Ulsan College of Medicine, Seoul, Republic of Korea

Objective: The prognostic value of coronary artery calcium (CAC) volume and density was derived from an automated artificial intelligence (AI)-based analysis of non-electrocardiogram-gated chest CT.

Materials and Methods: In this retrospective study, 7,552 asymptomatic adults who underwent chest CT as part of a national health screening program between 2007 and 2014 at two tertiary hospitals were examined for eligibility, of whom 1,109 with detectable CAC were analyzed. CAC density was derived by back-calculation from the Agatston score and CAC volume, both of which were obtained using AI software on chest CT. Differences in the probability of being free from major adverse cardiovascular events (MACE) across the four combined CAC volume-density groups were assessed using Kaplan–Meier curves and restricted mean survival time (RMST). Multivariable Cox proportional hazards models were used to assess the association between CAC volume and density and MACE.

Results: Among the 1,109 participants with nonzero CAC (median age, 60.3 years; 87% men), 207 experienced MACE during a median follow-up of 7.7 years. Ten-year RMSTs were 9.45 years in the low-volume-high-density group, 9.07 years in the low-volume-low-density group, 8.03 years in the high-volume-high-density group, and 7.68 years in the high-volume-low-density group. Differences in time to MACE were predominantly driven by CAC volume, with no significant density-related differences within the volume strata. CAC density demonstrated a significant, independent, inverse association after adjusting for CAC volume and clinical covariates (hazard ratio [HR] per increase by standard deviation [SD], 0.786; 95% confidence interval [CI], 0.659–0.936; $P = 0.007$). CAC volume also remained independently associated with an increased risk of MACE (HR per increase by SD, 2.608; 95% CI, 2.016–3.374; $P < 0.001$).

Conclusion: CAC density derived from chest CT using automated AI quantification was independently and inversely associated with MACE, providing additional prognostic value when added to CAC volume.

Keywords: Coronary artery; Calcium; Density; Plaque composition; Artificial intelligence

Received: October 25, 2025 **Revised:** March 22, 2026 **Accepted:** March 23, 2026

Corresponding author: Jong Eun Lee, MD, PhD, Department of Radiology and Research Institute of Radiology, Asan Medical Center, University of Ulsan College of Medicine, 88 Olympic-ro 43-gil, Songpa-gu, Seoul 05505, Republic of Korea
• E-mail: rollycandy2@naver.com
Corresponding author: Young Joo Suh, MD, PhD, Department of Radiology, Research Institute of Radiological Science, Severance Hospital, Yonsei University College of Medicine, 50-1 Yonsei-ro, Seodaemun-gu, Seoul 03722, Republic of Korea
• E-mail: rongzusuh@gmail.com

Korean Journal of Radiology
KJR

INTRODUCTION

The coronary artery calcium (CAC) score is a robust predictor of atherosclerotic cardiovascular disease events and informs preventive therapy decisions in individuals at intermediate risk [1,2]. The Agatston score is the most widely used CAC metric in clinical practice because of its ease of use in postprocessing and calculation. For each plaque, the Agatston score is determined by multiplying the lesion area by a density weighting factor, which is assigned from 1 to 4 based on peak attenuation in Hounsfield units (HU) [3].

The calcium density, which reflects the concentration of calcium within an atherosclerotic plaque, directly influences the Agatston score [4]. Although the Agatston score is a well-established risk predictor, several population-based cohort studies using cardiac CT have shown that higher calcium density is independently associated with a lower risk of cardiovascular events [5-10].

CAC can also be detected and quantified using non-electrocardiogram (ECG)-gated chest CT, with previous studies demonstrating strong concordance with dedicated ECG-gated calcium-scoring CT, thereby confirming its prognostic value [11-16]. With the increasing use of chest CT for lung cancer screening, artificial intelligence (AI)-based CAC quantification offers opportunities for opportunistic screening and timely preventive interventions [17-22]. However, the feasibility and prognostic value of CAC density derived from chest CT remain not well established.

In this study, we evaluated the association between CAC volume, density, and cardiovascular events using fully automated AI-based quantification of non-ECG-gated chest CTs performed as part of health screening at two medical centers.

MATERIALS AND METHODS

This retrospective study was approved by the Institutional Review Boards of two hospitals in South Korea, Severance Hospital (Center A) and Chonnam National University Hospital (Center B), both of which waived the requirement for written informed consent (IRB No. 4-2023-0985 at Center A and IRB No. CNUH-2023–303 at Center B).

Study Population

A total of 7,552 adults aged 40 years or older who underwent chest CT as part of a national health screening program between January 2007 and December 2014 were examined for eligibility (5,111 from Center A and 2,441 from Center B). Of these, 2,577 were excluded due to having less than 6 months of follow-up (n = 2,062), missing clinical data (n = 367), history of cardiovascular disease (n = 122), or segmentation failure (n = 26). Among the remaining 4,975 participants, 3,866 had no CAC (Agatston

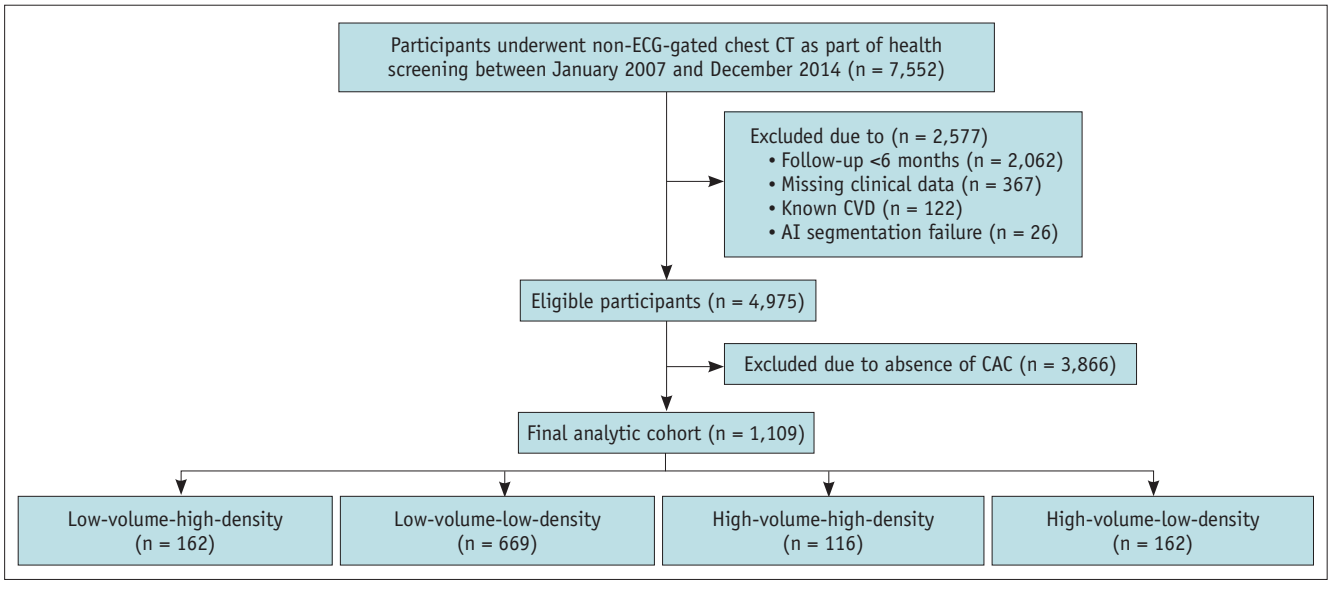

Fig. 1. Flowchart of the study population selection and group stratification. Participants were stratified into four groups according to CAC volume and CAC density, categorized as high (top quartile) or low (lower three quartiles). The top-quartile cutoffs were 173 mm^3 for CAC volume and 3.4 for CAC density. CAC = coronary artery calcium, ECG = electrocardiogram, CVD = cardiovascular disease, AI = artificial intelligence

https://doi.org/10.3348/kjr.2025.1614

score of 0) based on visual assessment or AI-based Agatston scoring and were excluded since the CAC density could not be calculated without detectable calcification. The final analytic cohort comprised 1,109 participants with non-zero CAC (Fig. 1).

All 1,109 participants were included in a previous study that investigated the prognostic value of thoracic aortic calcification and CAC using the Agatston score; however, neither CAC volume nor density was evaluated [23].

All the CT scans were acquired without ECG gating and without contrast. Slice thickness was 1.0 or 1.25 mm in Center A, and 3.0, 3.8, or 5.0 mm in Center B. Detailed acquisition parameters are summarized in Supplementary Table 1.

AI-Based CAC Quantification

Automated CAC quantification was performed using commercially available software (ClariCardio, version 1.0; ClariPi, Seoul, South Korea), which employs convolutional neural networks to segment the coronary arteries and calculate the Agatston score and CAC volume. Agatston scores were generated using the standard 130-HU threshold with automatic slice thickness correction standardized to a 3-mm reference. Validation demonstrated high agreement with manual measurements, with a concordance correlation coefficient of 0.895 [23,24].

Because the software does not provide per-lesion HU values, the CAC density score was back-calculated by dividing the Agatston score by the total CAC area (calculated as CAC volume divided by slice thickness), which is consistent with previous studies [5,6,8-10]. This yielded a dimensionless Agatston-derived density factor (range, 1–4) reflecting the participant-level average peak density, hereafter referred to as the CAC density.

Risk Factors and Participant Outcomes

Baseline clinical data, including age, sex, body mass index, medical history, and laboratory findings, were obtained from electronic medical records. The occurrence of major adverse cardiovascular events (MACE), a composite of unstable angina requiring hospitalization or revascularization, myocardial infarction, ischemic stroke, and cardiovascular death, was confirmed, and the time to first MACE was calculated by reviewing electronic medical records. Events were adjudicated until December 31, 2023. Participants without MACE were censored at the last recorded clinical encounter. A minimum follow-up of six months post-CT was required.

Statistical Analysis

Skewed variables (Agatston score, CAC area, and CAC volume) were log-transformed using natural logarithms. Descriptive statistics were compared using the Wilcoxon rank-sum test or the χ^2 test. Spearman's correlation coefficients were used to evaluate the relationships among the CAC measures.

To evaluate the joint prognostic value of CAC volume and density, the participants were stratified into four groups based on whether their CAC volume and density fell within the top quartile (high volume or high density) or the lower three quartiles (low volume or low density). The probability of being free from MACE was estimated using the Kaplan–Meier method, and pairwise comparisons of the Kaplan–Meier curves were conducted using the log-rank test with Bonferroni correction.

To quantify event-free time, the restricted mean survival time (RMST) was calculated at 5 and 10 years using the trapezoidal rule without assuming a parametric survival distribution. The RMST represents the area under the Kaplan–Meier curve within a defined follow-up period (e.g., a 5-year RMST of four years indicates that a participant remained free of MACE for four years within five years after baseline) [25]. RMST estimates, pairwise differences, 95% confidence intervals (CIs), and *P*-values were obtained using 1,000 bootstrap replicates before and after inverse probability of treatment weighting (IPTW). For the IPTW-adjusted analyses, generalized propensity scores were estimated using multinomial logistic regression, adjusting for all baseline covariates. Stabilized IPTW weights were calculated, and the covariate balance was evaluated using standardized mean differences. After weighting, all covariates achieved adequate balance, with standardized mean differences of <0.1 across all variables (Supplementary Table 2).

Univariable and multivariable Cox proportional hazards regression analyses were performed to evaluate the association between CAC measures and MACE. The full model included CAC volume, CAC density, and clinical covariates, while excluding Agatston score and CAC area to avoid multicollinearity. The proportional hazards assumption was evaluated using Schoenfeld residuals, and time-varying coefficient Cox models were applied to any violations (Supplementary Table 3). Sensitivity analyses were performed for the subgroups defined by consistent CT acquisition parameters.

https://doi.org/10.3348/kjr.2025.1614

Korean Journal of Radiology
KJR

All statistical analyses were performed using R software (version 4.2.1; R Foundation for Statistical Computing, Vienna, Austria). A *P*-value <0.05 was considered statistically significant, except for pairwise comparisons among the four groups using the log-rank test and RMST analyses, for which a Bonferroni-adjusted significance threshold ($P < 0.008$) was applied.

RESULTS

Baseline Characteristics

The median age of the 1,109 participants was 60.3 years (interquartile range, 55.0–66.9 years), and 965 (87%) were men. The median follow-up was 7.7 years (8,598 person-years), during which 207 participants experienced MACE.

Table 1 summarizes the baseline characteristics, with comparisons between the top quartile (quartile 4) and the lower quartiles (quartiles 1–3) for both CAC volume and density. The cutoff for the top quartile was 173 mm^3 for CAC volume and 3.4 for CAC density.

Participants in the top-volume quartile were older and had a higher prevalence of hypertension, diabetes, and dyslipidemia. They also had significantly lower body mass index, total cholesterol, and low-density lipoprotein (LDL) cholesterol levels, whereas high-density lipoprotein (HDL) cholesterol levels did not differ. The MACE incidence in the top-volume quartile was 47.5 per 1,000 person-years versus 21.5 in the lower quartiles ($P < 0.001$). When stratified by CAC density, participants in the top-density quartile were older and had lower total and LDL cholesterol levels. The MACE incidence in the top-density quartile was 24.7 per 1,000 person-years versus 28.3 in the lower quartiles ($P = 0.422$).

Correlation Among CAC Measures

The log-transformed Agatston score, CAC area, and CAC volume showed very strong correlations (Spearman's $\rho > 0.9$) (Supplementary Table 4). In contrast, CAC density was only moderately correlated with the other three measures (Spearman's $\rho = 0.644$, 0.617, and 0.518 for Agatston score, CAC area, and CAC volume, respectively).

Occurrence of MACE by Combined CAC Volume and Density

Participants were stratified into four groups based on the top quartile cutoff for CAC volume and density: 162 in the low-volume-high-density group, 669 in the low-volume-low-density group, 116 in the high-volume-high-density group, and 162 in the high-volume-low-density group (Figs. 1, 2). The Kaplan–Meier curves of the probability of freedom from MACE showed clear differences among the four groups over time (Fig. 3). Differences in MACE risk were primarily driven

Table 1. Baseline characteristics of study participants by CAC volume and density

Variables	Grouping by CAC volume			Grouping by CAC density		
	Quartiles 1–3 (n = 832)	Quartile 4 (n = 277)	*P*	Quartiles 1–3 (n = 832)	Quartile 4 (n = 277)	*P*
Age, yr	59.0 (53.8–65.2)	64.6 (59.5–71.0)	<0.001	60.0 (54.8–66.5)	61.3 (55.9–68.1)	0.029
Sex, male	716 (86.1)	249 (89.9)	0.174	725 (87.1)	240 (86.6)	0.773
BMI, kg/m^2	24.4 (22.5–26.3)	23.9 (22.1–26.0)	0.028	24.3 (22.5–26.2)	24.2 (22.1–26.3)	0.443
Hypertension	279 (33.5)	133 (48.0)	<0.001	313 (37.6)	99 (35.7)	0.575
Diabetes	148 (17.8)	82 (29.6)	<0.001	163 (19.6)	67 (24.2)	0.102
Dyslipidemia	87 (10.5)	42 (15.2)	0.034	94 (11.3)	35 (12.6)	0.548
Total cholesterol, mg/dL	194.0 (171.0–219.0)	181.0 (154.7–207.0)	<0.001	193.0 (169.0–218.5)	188.0 (159.0–210.0)	0.010
HDL-C, mg/dL	47.0 (40.0–55.0)	47.0 (40.0–56.0)	0.738	47.0 (40.0–55.0)	47.0 (41.0–56.0)	0.214
LDL-C, mg/dL	121.5 (99.0–143.0)	109.0 (81.0–133.0)	<0.001	121.0 (96.0–143.0)	113.0 (87.0–134.0)	<0.001
Ever smoker	600 (72.1)	205 (74.0)	0.541	607 (72.9)	198 (71.5)	0.917
MACE per 1,000 person-years	21.5	47.5	<0.001	28.3	24.7	0.422
Agatston score	31.7 (11.1–71.3)	396.9 (264.5–693.7)	<0.001	35.6 (11.2–114.0)	153.8 (62.7–410.1)	<0.001
CAC volume, mm^3	36.7 (14.4–76.0)	369.3 (250.8–610.4)	<0.001	47.3 (16.1–127.9)	124.5 (52.8–355.7)	<0.001
CAC density	2.6 (2.0–3.2)	3.3 (3.0–3.6)	<0.001	2.5 (2.0–3.0)	3.6 (3.5–3.8)	<0.001

Data are presented as medians with interquartile ranges in parentheses for continuous variables and as numbers with percentages in parentheses for categorical variables. CAC density is a dimensionless Agatston-derived factor (range, 1–4), reflecting the participant-level average peak density. The cutoff values for the top quartiles were 173 mm^3 for CAC volume and 3.4 for CAC density.
CAC = coronary artery calcium, BMI = body mass index, HDL-C = high-density lipoprotein cholesterol, LDL-C = low-density lipoprotein cholesterol, MACE = major adverse cardiovascular events

 https://doi.org/10.3348/kjr.2025.1614

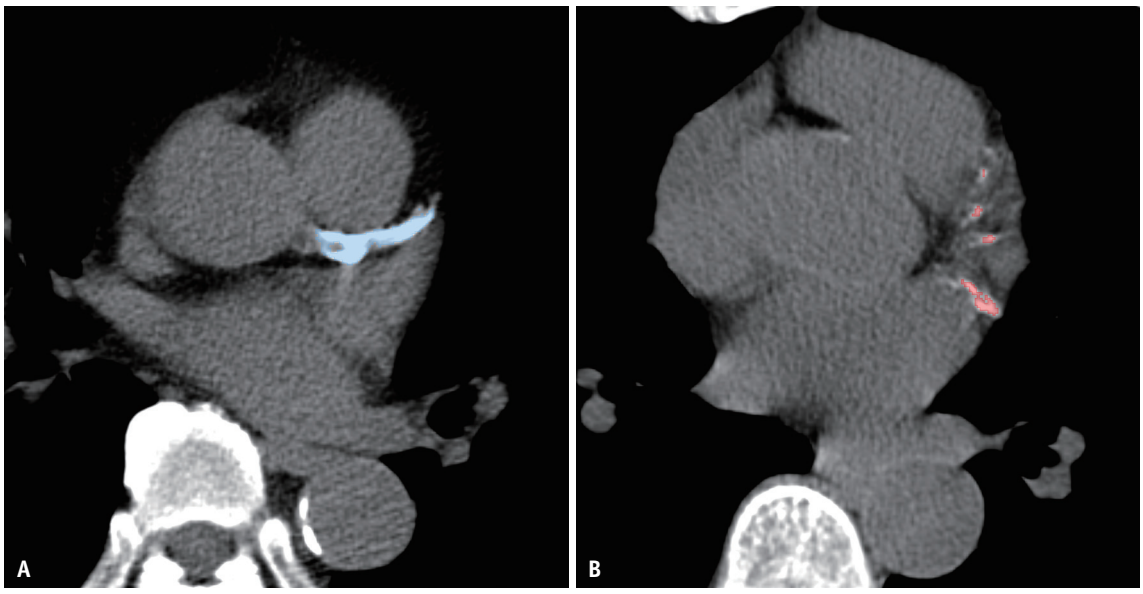

Fig. 2. Representative cases of CAC with high and low densities. **A:** High-volume-high-density CAC in a 65-year-old male, showing diffuse calcification from the left main to the left anterior descending artery (blue areas). The Agatston score was 2,978, CAC volume was 2,343 mm^3, and density was 3.8. The participant did not experience MACE during the follow-up period of 3,291 days. **B:** High-volume-low-density CAC in a 70-year-old male, showing scattered calcifications in the left anterior descending artery, diagonal branch, ramus intermedius, and left circumflex artery (red areas). The Agatston score was 853, CAC volume was 967 mm^3, and density was 2.6. The participant experienced MACE 3,156 days after the baseline CT scan. CAC = coronary artery calcium, MACE = major adverse cardiovascular events

by CAC volume rather than CAC density. The low-volume-high-density group exhibited the most favorable prognosis, showing a significantly longer time to MACE than the high-volume-low-density group (log-rank $P < 0.001$) and a marginally longer time than the high-volume-high-density group (log-rank $P = 0.011$). No significant differences were observed between groups within the same volume category (log-rank $P = 1.00$ for both comparisons).

Table 2 presents the RMST estimates at 5 and 10 years across the four groups. At 5 and 10 years, pairwise comparisons showed no statistically significant differences between the two high-volume groups ($P = 0.946$ at 5 years and $P = 0.450$ at 10 years) or between the two low-volume groups ($P = 0.018$ at 5 years and $P = 0.038$ at 10 years), whereas all other between-group comparisons were statistically significant ($P < 0.008$). Overall, the differences in RMST were predominantly driven by CAC volume. Within each volume stratum, higher CAC density was associated with higher RMST; yet these differences were not statistically significant. The RMST estimates remained largely consistent after IPTW adjustment, with the relative group rankings preserved.

Association of CAC Measures With MACE

Table 3 presents the results of the Cox proportional hazards regression analyses for MACE. In the univariable analysis, the log-transformed Agatston score, CAC area, and CAC volume were associated with an increased risk of MACE. Each score showed a time-dependent interaction (hazard ratio [HR] <1), suggesting that its association with MACE diminished over time. In contrast, CAC density was not significantly associated with MACE in univariable analysis. In the multivariable analysis adjusted for clinical covariates, CAC density showed a significant inverse association with MACE (HR per standard deviation [SD], 0.786; 95% CI, 0.659–0.936; $P = 0.007$), while CAC volume remained independently associated with an increased risk of MACE (HR per SD, 2.608; 95% CI, 2.016–3.374; $P < 0.001$).

A restricted cubic spline curve revealed a nonlinear relationship between CAC volume and MACE risk, with the greatest increase in HR observed between Z-scores of 1 and 2 (Fig. 4A). The time-interaction term for CAC volume yielded an HR of 0.922 per year (per SD), indicating that the relative risk associated with volume decreased by approximately 7.8% annually, reflecting time-dependent attenuation of risk (Fig. 4B). For CAC density, the adjusted model revealed a clear inverse association with MACE risk, not observed in the unadjusted model (Fig. 4C, D).

Sensitivity Analyses

Sensitivity analyses restricted to subgroups with uniform

https://doi.org/10.3348/kjr.2025.1614

Korean Journal of Radiology
KJR

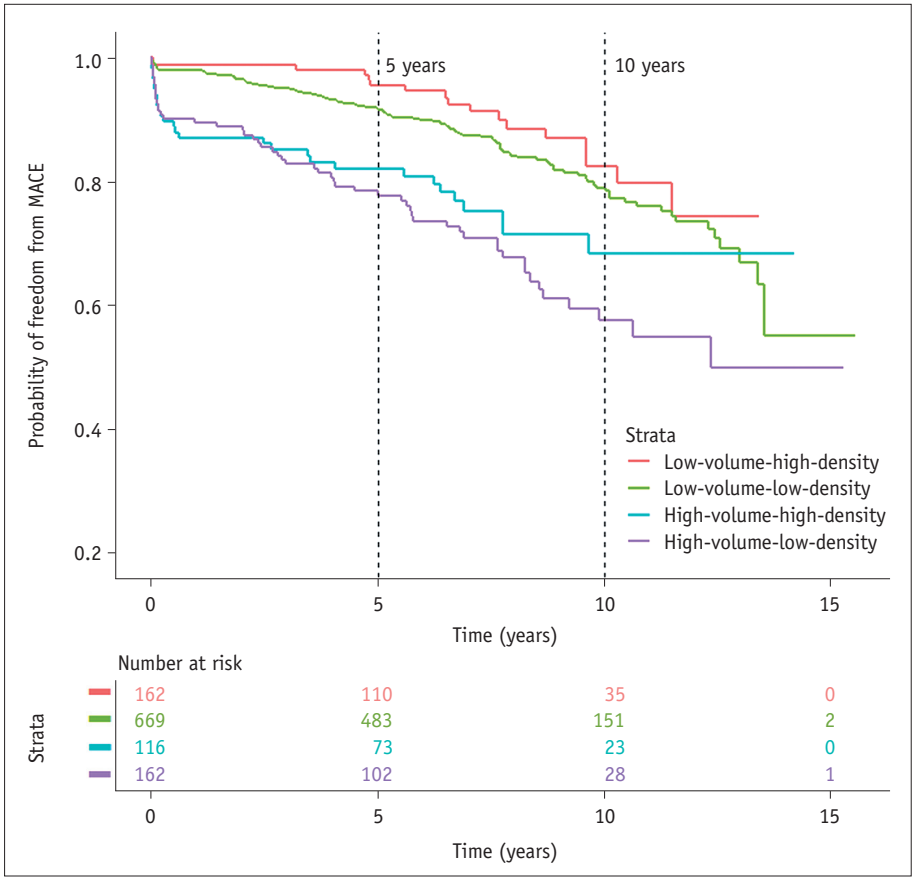

Fig. 3. Kaplan–Meier curves for the probability of freedom from MACE stratified by CAC volume and density. High CAC volume and density were defined as values within the top quartile of each respective measure (≥173 mm^3 for CAC volume and ≥3.4 for CAC density). The number at risk at selected time points is displayed below the x-axis. The truncation times for calculating the restricted mean survival times were 5 and 10 years. MACE = major adverse cardiovascular events, CAC = coronary artery calcium

Table 2. RMST across CAC volume-density groups

Groups	5-year RMST		10-year RMST	
	Unweighted	Weighted	Unweighted	Weighted
Low-volume-high-density	4.92 (4.83–4.99)	4.92 (4.80–4.99)	9.45 (9.14–9.70)	9.45 (9.13–9.72)
Low-volume-low-density	4.77 (4.70–4.84)	4.77 (4.70–4.84)	9.07 (8.87–9.25)	9.08 (8.88–9.27)
High-volume-high-density	4.28 (3.97–4.56)	4.38 (4.04–4.65)	8.03 (7.35–8.69)	8.33 (7.59–8.95)
High-volume-low-density	4.27 (4.02–4.49)	4.31 (4.04–4.54)	7.68 (7.09–8.21)	7.85 (7.24–8.40)

Values are presented as RMST in years, with 95% confidence intervals in parentheses. The results are shown for both unweighted and weighted analyses, with the latter incorporating inverse probability of treatment weighting. The 5-year RMST of 4.92 years in the low-volume-high-density group indicates that individuals in this group remained free of MACE for approximately 4.92 of the 5 years following baseline.
RMST = restricted mean survival time, CAC = coronary artery calcium, MACE = major adverse cardiovascular events

CT acquisition parameters demonstrated a consistent inverse association between CAC density and MACE risk (Supplementary Table 5). As in the full cohort, this association persisted across participants scanned with a standard reconstruction kernel (n = 1,015), at 120 kVp (n = 865), with 1–3 mm slice thickness (n = 998), or with 1 mm slice thickness (n = 660), with multivariable HRs of 0.819, 0.728, 0.738, and 0.688, respectively (all $P < 0.05$).

DISCUSSION

In this health-screening population study, CAC density derived from non-ECG-gated chest CT was significantly associated with a lower risk of MACE after adjusting for CAC

 https://doi.org/10.3348/kjr.2025.1614

Table 3. Cox proportional hazards regression analysis for MACE

CAC measure	Univariable analysis		Multivariable analysis*	
	HR (95% CI), per SD	*P*	HR (95% CI), per SD	*P*
ln(Agatston)	2.182 (1.721–2.767)	<0.001		
Time interaction term for ln(Agatston)	0.924 (0.887–0.962)	<0.001		
ln(Area)	1.807 (1.452–2.248)	<0.001		
Time interaction term for ln(Area)	0.944 (0.907–0.983)	0.005		
ln(Volume)	2.365 (1.862–3.000)	<0.001	2.608 (2.016–3.374)	<0.001
Time interaction term for ln(Volume)	0.916 (0.879–0.955)	<0.001	0.922 (0.884–0.961)	<0.001
Density	1.045 (0.910–1.200)	0.531	0.786 (0.659–0.936)	0.007

HR values were calculated for an increase by SD. Schoenfeld residuals indicated violation of the proportional hazards assumption for ln(Agatston), ln(Area), and ln(Volume) (see Supplementary Table 3); consequently, time-varying coefficient Cox models were used for these variables.
*The multivariable analysis included CAC volume, CAC density, and clinical covariates (age, sex, body mass index, hypertension, diabetes, dyslipidemia, smoking, high-density lipoprotein cholesterol, low-density lipoprotein cholesterol, blood urea nitrogen, and creatinine). For simplicity, the results for clinical covariates are not shown.
MACE = major adverse cardiovascular events, HR = hazard ratio, SD = standard deviation, CAC = coronary artery calcium, CI = confidence interval

volume (adjusted HR per SD, 0.786), corresponding to a 21.4% lower risk per SD increase. In time-to-event analyses, differences in time to MACE were primarily determined by CAC volume, whereas CAC density provided an additional but non-significant prognostic separation within the volume strata.

Multiple cohort studies have shown that the prognostic value of CAC density becomes apparent only when the overall plaque burden is considered. In MESA, the CAC Consortium, and subsequent meta-analyses, CAC density demonstrated no significant or positive associations with cardiovascular events when models were adjusted solely for demographic or clinical variables [5,6,8,9,26-28]. Individuals with higher CAC density tend to be older and have a greater plaque burden, resulting in a moderate density–volume correlation, as observed in previous studies and in ours [9,27,29]. Such shared variance can obscure the inverse association between density and outcomes in unadjusted models. However, after formal adjustment for CAC volume, higher CAC density was consistently correlated with lower cardiovascular event risk, supporting the concept that denser calcification reflects a more stable plaque [27]. A recent meta-analysis reaffirmed this relationship: higher CAC density was associated with a 20% lower risk of cardiovascular events per SD increase only in models adjusted for CAC volume [28]. Our findings are consistent with these observations and extend the prior evidence of the prognostic implications of CAC density in an independent Asian health-screening cohort using AI-based quantification from non-ECG-gated chest CT.

Our RMST analyses evaluating the joint prognostic value of CAC volume and density indicated that CAC volume was the primary determinant of prognosis. Although CAC density showed a modest, non-significant modifying effect within each volume stratum in our rigorously adjusted analyses, a consistent directional trend was observed. Prior studies have shown that the prognostic value of CAC density is most evident in low-burden populations [8-10]. This volume-dependent prognostic effect of CAC density may partly reflect the limited dynamic range of the Agatston-derived density factor, which caps higher-density plaques at a maximum value of four, particularly in individuals with high plaque burden. However, the persistence of volume-dependent effects, even in studies using direct HU-based density measurements, suggests that this phenomenon cannot be explained solely by metric limitations [9]. In individuals with extensive calcified plaques, CAC volume itself may act as a dominant risk enhancer, thereby attenuating the incremental prognostic contribution of CAC density [5-10,29-31]. Meanwhile, the observed attenuation of the hazard associated with CAC volume over follow-up is consistent with prior observations in asymptomatic screening cohorts, where baseline plaque burden strongly predicts early events, yet its relative prognostic impact diminishes over longer follow-up as competing risk factors, medical treatments, and risk modification accumulate [32-34].

The prognostic relevance of CAC density derived from chest CT images using automated AI-based quantification remains to be established. Naghavi et al. [35] recently applied AI to ECG-gated CAC scoring scans and reported improved outcome prediction using plaque characteristics,

https://doi.org/10.3348/kjr.2025.1614

Korean Journal of Radiology
KJR

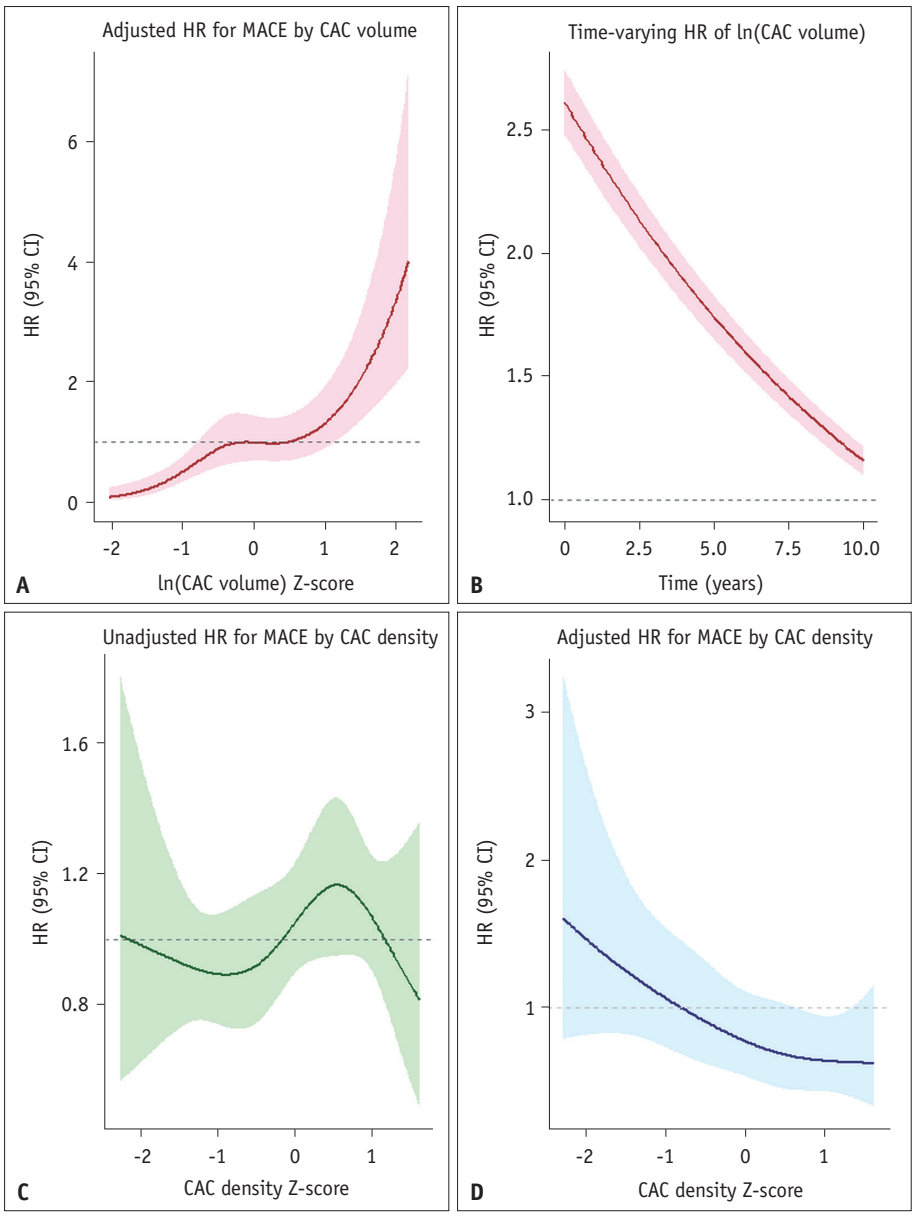

Fig. 4. Restricted cubic spline plots for HRs for MACE according to CAC volume and density. **A:** Adjusted HRs for MACE across the range of log-transformed CAC volume (Z-scores). **B:** Time-varying HRs for log-transformed CAC volume estimated from a Cox model with a time interaction term. The HR at time *t* is modeled as: HR(*t*) = 2.608 x 0.922*t*. **C, D:** Unadjusted and adjusted HRs across the range of CAC density, respectively. HR = hazard ratio, MACE = major adverse cardiovascular events, CAC = coronary artery calcium, CI = confidence interval

including density and distribution. As incidental CAC becomes increasingly relevant in routine chest CT scans, AI may enhance its use in opportunistic cardiovascular risk stratification. Our findings support the feasibility of deriving CAC volume and density from chest CT scans and underscore the importance of interpreting these metrics together. If validated in larger cohorts, this approach may reduce the need for dedicated CAC-scoring CT scans in screening programs.

We used the average peak density calculated as the Agatston score divided by the total plaque area. Although this metric does not represent lesion-level "true density," it reasonably reflects the patient-level tendency toward denser or less dense calcification and can be derived from routinely available variables (Agatston score, volume, and slice thickness). This back-calculated density metric was also used in several foundational studies, in which it consistently demonstrated an inverse association with cardiovascular outcomes [5,6,8,9]. While the direct measurement of HU offers greater precision, manual or

 https://doi.org/10.3348/kjr.2025.1614

semi-automated quantification is time-consuming and prone to inter-observer variability. These limitations highlight the need for AI-driven HU-based density metrics and their systematic validation.

The acquisition parameters critically influence CAC measurements. Slice thickness affects the detection of small lesions through partial volume effects and alters image noise [36], whereas lower kVp settings increase calcium attenuation, potentially necessitating higher HU thresholds than the standard 130 HU [37]. Despite some variability, most examinations in this study were performed under relatively consistent parameters: predominantly 1–3 mm slice thickness, 120 kVp, and a standard reconstruction kernel. Moreover, the AI software accounts for this variability by normalizing the Agatston scores to a 3-mm reference standard. Sensitivity analyses restricted to uniform acquisition parameters consistently demonstrated an inverse association between CAC density and MACE. Future studies should systematically evaluate the effect of acquisition parameters on AI-based CAC quantification and cardiovascular risk reclassification.

This study has several limitations. First, CAC density was derived as a participant-level, area-weighted, Agatston-based metric rather than as a direct lesion-level HU measurement. Accordingly, it does not capture lesion-level heterogeneity or mixed calcification patterns. Secondly, lipid-lowering therapy, a potential confounder affecting CAC measures and outcomes, could not be reliably assessed. Third, the CT acquisition parameters were not fully homogeneous across centers. Fourth, outcome ascertainment relied on institutional electronic medical records without linkage to national claims data, potentially leading to the under-ascertainment of events occurring outside institutions. However, this limitation is likely to be non-differential, generally biasing the results toward the null. Lastly, participants with less than six months of follow-up were excluded to ensure reliable outcome ascertainment, potentially introducing retention bias.

In conclusion, CAC density derived from non-ECG-gated chest CT using automated AI quantification was independently and inversely associated with cardiovascular events. The combined interpretation of CAC volume and density may provide a more nuanced assessment of cardiovascular risk beyond the Agatston score alone and holds promise for opportunistic risk assessment using routine chest CT scans.

Supplement

The Supplement is available with this article at https://doi.org/10.3348/kjr.2025.1614.

Availability of Data and Material

The datasets generated or analyzed during the study are available from the corresponding author on reasonable request.

Conflicts of Interest

The authors have no potential conflicts of interest to disclose.

Author Contributions

Conceptualization: Na Young Kim, Jong Eun Lee, Young Joo Suh. Data curation: Jong Eun Lee, Yun-Hyeon Kim, Young Joo Suh. Formal analysis: Na Young Kim. Funding acquisition: Young Joo Suh. Investigation: Na Young Kim. Methodology: Na Young Kim. Supervision: Jong Eun Lee, Young Joo Suh. Validation: Jong Eun Lee, Young Joo Suh. Visualization: Na Young Kim. Writing—original draft: Na Young Kim. Writing—review & editing: Na Young Kim, Jong Eun Lee, Yun-Hyeon Kim, Young Joo Suh.

ORCID IDs

Na Young Kim
https://orcid.org/0000-0003-1645-2434
Yun-Hyeon Kim
https://orcid.org/0000-0002-0047-0729
Jong Eun Lee
https://orcid.org/0000-0002-8754-6801
Young Joo Suh
https://orcid.org/0000-0002-2078-5832

Funding Statement

This research was supported by National Research Foundation of Korea (NRF) grant funded by the Korea government (MSIT) (No. 2021R1A2C4002195).

Acknowledgments

We thank Kyunghwa Han, PhD, a statistician at the Department of Radiology, Research Institute of Radiological Science, Yonsei University College of Medicine, for her assistance with statistical interpretation of the data.

Korean Journal of Radiology
KJR

REFERENCES

1. Grundy SM, Stone NJ, Bailey AL, Beam C, Birtcher KK, Blumenthal RS, et al. 2018 AHA/ACC/AACVPR/AAPA/ABC/ACPM/ADA/AGS/APhA/ASPC/NLA/PCNA guideline on the management of blood cholesterol: a report of the American College of Cardiology/American Heart Association Task Force on clinical practice guidelines. *J Am Coll Cardiol* 2019;73:e285-e350
2. Arnett DK, Blumenthal RS, Albert MA, Buroker AB, Goldberger ZD, Hahn EJ, et al. 2019 ACC/AHA guideline on the primary prevention of cardiovascular disease: a report of the American College of Cardiology/American Heart Association Task Force on clinical practice guidelines. *Circulation* 2019;140:e596-e646
3. Agatston AS, Janowitz WR, Hildner FJ, Zusmer NR, Viamonte M Jr, Detrano R. Quantification of coronary artery calcium using ultrafast computed tomography. *J Am Coll Cardiol* 1990;15:827-832
4. Blaha MJ, Mortensen MB, Kianoush S, Tota-Maharaj R, Cainzos-Achirica M. Coronary artery calcium scoring: is it time for a change in methodology? *JACC Cardiovasc Imaging* 2017;10:923-937
5. Criqui MH, Denenberg JO, Ix JH, McClelland RL, Wassel CL, Rifkin DE, et al. Calcium density of coronary artery plaque and risk of incident cardiovascular events. *JAMA* 2014;311:271-278
6. Criqui MH, Knox JB, Denenberg JO, Forbang NI, McClelland RL, Novotny TE, et al. Coronary artery calcium volume and density: potential interactions and overall predictive value: the multi-ethnic study of atherosclerosis. *JACC Cardiovasc Imaging* 2017;10:845-854
7. Shaw LJ, Min JK, Nasir K, Xie JX, Berman DS, Miedema MD, et al. Sex differences in calcified plaque and long-term cardiovascular mortality: observations from the CAC consortium. *Eur Heart J* 2018;39:3727-3735
8. Osei AD, Mirbolouk M, Berman D, Budoff MJ, Miedema MD, Rozanski A, et al. Prognostic value of coronary artery calcium score, area, and density among individuals on statin therapy vs. non-users: the coronary artery calcium consortium. *Atherosclerosis* 2021;316:79-83
9. Dzaye O, Razavi AC, Dardari ZA, Berman DS, Budoff MJ, Miedema MD, et al. Mean versus peak coronary calcium density on non-contrast CT: calcium scoring and ASCVD risk prediction. *JACC Cardiovasc Imaging* 2022;15:489-500
10. Bhatia HS, McClelland RL, Denenberg J, Budoff MJ, Allison MA, Criqui MH. Coronary artery calcium density and cardiovascular events by volume level: the MESA. *Circ Cardiovasc Imaging* 2023;16:e014788
11. Wu MT, Yang P, Huang YL, Chen JS, Chuo CC, Yeh C, et al. Coronary arterial calcification on low-dose ungated MDCT for lung cancer screening: concordance study with dedicated cardiac CT. *AJR Am J Roentgenol* 2008;190:923-928
12. Jacobs PC, Gondrie MJ, Mali WP, Oen AL, Prokop M, Grobbee DE, et al. Unrequested information from routine diagnostic chest CT predicts future cardiovascular events. *Eur Radiol* 2011;21:1577-1585
13. Hughes-Austin JM, Dominguez A 3rd, Allison MA, Wassel CL, Rifkin DE, Morgan CG, et al. Relationship of coronary calcium on standard chest CT scans with mortality. *JACC Cardiovasc Imaging* 2016;9:152-159
14. Hecht HS, Cronin P, Blaha MJ, Budoff MJ, Kazerooni EA, Narula J, et al. 2016 SCCT/STR guidelines for coronary artery calcium scoring of noncontrast noncardiac chest CT scans: a report of the Society of Cardiovascular Computed Tomography and Society of Thoracic Radiology. *J Cardiovasc Comput Tomogr* 2017;11:74-84
15. Chen Y, Hu Z, Li M, Jia Y, He T, Liu Z, et al. Comparison of nongated chest CT and dedicated calcium scoring CT for coronary calcium quantification using a 256-dector row CT scanner. *Acad Radiol* 2019;26:e267-e274
16. Kim JY, Suh YJ, Han K, Choi BW. Reliability of coronary artery calcium severity assessment on non-electrocardiogram-gated CT: a meta-analysis. *Korean J Radiol* 2021;22:1034-1043
17. Takx RA, de Jong PA, Leiner T, Oudkerk M, de Koning HJ, Mol CP, et al. Automated coronary artery calcification scoring in non-gated chest CT: agreement and reliability. *PLoS One* 2014;9:e91239
18. van Velzen SGM, Lessmann N, Velthuis BK, Bank IEM, van den Bongard DHJG, Leiner T, et al. Deep learning for automatic calcium scoring in CT: validation using multiple cardiac CT and chest CT protocols. *Radiology* 2020;295:66-79
19. Zeleznik R, Foldyna B, Eslami P, Weiss J, Alexander I, Taron J, et al. Deep convolutional neural networks to predict cardiovascular risk from computed tomography. *Nat Commun* 2021;12:715
20. Eng D, Chute C, Khandwala N, Rajpurkar P, Long J, Shleifer S, et al. Automated coronary calcium scoring using deep learning with multicenter external validation. *NPJ Digit Med* 2021;4:88
21. Kang HW, Ahn WJ, Jeong JH, Suh YJ, Yang DH, Choi H, et al. Evaluation of fully automated commercial software for Agatston calcium scoring on non-ECG-gated low-dose chest CT with different slice thickness. *Eur Radiol* 2023;33:1973-1981
22. Sandhu AT, Rodriguez F, Ngo S, Patel BN, Mastrodicasa D, Eng D, et al. Incidental coronary artery calcium: opportunistic screening of previous nongated chest computed tomography scans to improve statin rates (NOTIFY-1 project). *Circulation* 2023;147:703-714
23. Lee JE, Kim NY, Kim YH, Kwon Y, Kim S, Han K, et al. Long-term prognostic implications of thoracic aortic calcification on CT using artificial intelligence–based quantification in a screening population: a two-center study. *AJR Am J Roentgenol* 2025;224:e2532697
24. Kim S, Park EA, Ahn C, Jeong B, Lee YS, Lee W, et al. Performance of fully automated deep-learning-based coronary artery calcium scoring in ECG-gated calcium CT and non-gated low-dose chest CT. *Eur Radiol* 2025;35:7084-7095
25. Han K, Jung I. Restricted mean survival time for survival

 https://doi.org/10.3348/kjr.2025.1614

analysis: a quick guide for clinical researchers. *Korean J Radiol* 2022;23:495-499
26. Guo J, Erqou SA, Miller RG, Edmundowicz D, Orchard TJ, Costacou T. The role of coronary artery calcification testing in incident coronary artery disease risk prediction in type 1 diabetes. *Diabetologia* 2019;62:259-268
27. Razavi AC, Agatston AS, Shaw LJ, De Cecco CN, van Assen M, Sperling LS, et al. Evolving role of calcium density in coronary artery calcium scoring and atherosclerotic cardiovascular disease risk. *JACC Cardiovasc Imaging* 2022;15:1648-1662
28. Yong Y, Giovannucci J, Pang SN, Hong W, Han D, Berman DS, et al. Coronary artery calcium density and risk of cardiovascular events: a systematic review and meta-analysis. *JACC Cardiovasc Imaging* 2025;18:294-304
29. Foldyna B, Eslami P, Scholtz JE, Baltrusaitis K, Lu MT, Massaro JM, et al. Density and morphology of coronary artery calcium for the prediction of cardiovascular events: insights from the Framingham Heart Study. *Eur Radiol* 2019;29:6140-6148
30. Bellasi A, Ferramosca E, Ratti C, Block G, Raggi P. The density of calcified plaques and the volume of calcium predict mortality in hemodialysis patients. *Atherosclerosis* 2016;250:166-171
31. Mukai H, Dai L, Chen Z, Lindholm B, Ripsweden J, Brismar TB, et al. Inverse J-shaped relation between coronary arterial calcium density and mortality in advanced chronic kidney disease. *Nephrol Dial Transplant* 2020;35:1202-1211
32. Budoff MJ, Shaw LJ, Liu ST, Weinstein SR, Mosler TP, Tseng PH, et al. Long-term prognosis associated with coronary calcification: observations from a registry of 25,253 patients. *J Am Coll Cardiol* 2007;49:1860-1870
33. Nasir K, McClelland RL, Blumenthal RS, Goff DC Jr, Hoffmann U, Psaty BM, et al. Coronary artery calcium in relation to initiation and continuation of cardiovascular preventive medications: the multi-ethnic study of atherosclerosis (MESA). *Circ Cardiovasc Qual Outcomes* 2010;3:228-235
34. Rozanski A, Gransar H, Shaw LJ, Kim J, Miranda-Peats L, Wong ND, et al. Impact of coronary artery calcium scanning on coronary risk factors and downstream testing the EISNER (early identification of subclinical atherosclerosis by noninvasive imaging research) prospective randomized trial. *J Am Coll Cardiol* 2011;57:1622-1632
35. Naghavi M, Reeves AP, Atlas K, Zhang C, Atlas T, Henschke CI, et al. Artificial intelligence applied to coronary artery calcium scans (AI-CAC) significantly improves cardiovascular events prediction. *NPJ Digit Med* 2024;7:309
36. Mantini C, Maffei E, Toia P, Ricci F, Seitun S, Clemente A, et al. Influence of image reconstruction parameters on cardiovascular risk reclassification by computed tomography coronary artery calcium score. *Eur J Radiol* 2018;101:1-7
37. Nakazato R, Dey D, Gutstein A, Le Meunier L, Cheng VY, Pimentel R, et al. Coronary artery calcium scoring using a reduced tube voltage and radiation dose protocol with dual-source computed tomography. *J Cardiovasc Comput Tomogr* 2009;3:394-400

https://doi.org/10.3348/kjr.2025.1614